

Supporting Information

Table S1 Orthogonal experiment of HDTM micelles.

| Test | A | B | C | D | Size (nm) | EE of HYP | EE of DXM |
|----------------------------|--------|--------|--------|--------|--|-----------|-----------|
| 1 | 2.50% | 20% | 0.5 | 1 : 4 | 91.72 | 1 | 0.4 |
| 2 | 2.50% | 30% | 1 | 1 : 8 | 144.77 | 1 | 0.41 |
| 3 | 2.50% | 40% | 1.5 | 1 : 10 | 172.67 | 1 | 0.53 |
| 4 | 5.00% | 20% | 1 | 1 : 10 | 501 | 0.97 | 0.43 |
| 5 | 5.00% | 30% | 1.5 | 1 : 4 | 272.9 | 0.98 | 0.46 |
| 6 | 5.00% | 40% | 0.5 | 1 : 8 | 254.23 | 1 | 0.36 |
| 7 | 7.50% | 20% | 1.5 | 1 : 8 | 155 | 1 | 0.5 |
| 8 | 7.50% | 30% | 0.5 | 1 : 10 | 579.9 | 1 | 0.39 |
| 9 | 7.50% | 40% | 1 | 1 : 4 | 123.07 | 0.83 | 0.38 |
| Size | | | | | | | |
| K1 | 136.38 | 249.24 | 308.62 | 162.56 | Optimization levels | | |
| K2 | 342.71 | 332.52 | 256.28 | 184.67 | DABC | | |
| K3 | 285.99 | 183.32 | 200.19 | 417.85 | Optimal formulation for size | | |
| R | 206.33 | 149.2 | 108.43 | 255.29 | D1 A1 B3 C3 | | |
| EE of HYP | | | | | | | |
| T1 | 1 | 0.991 | 1 | 0.94 | Optimization levels | | |
| T2 | 0.986 | 0.995 | 0.936 | 1 | CDAB | | |
| T3 | 0.945 | 0.945 | 0.995 | 0.991 | Optimal formulation for EE of HYP | | |
| R | 0.055 | 0.05 | 0.064 | 0.06 | C1 D2 A1 B2 | | |
| EE of DXM | | | | | | | |
| Z1 | 0.447 | 0.443 | 0.383 | 0.41 | Optimization levels | | |
| Z2 | 0.417 | 0.42 | 0.407 | 0.427 | CDAB | | |
| Z3 | 0.423 | 0.423 | 0.5 | 0.45 | Optimal formulation for EE of DXM | | |
| R | 0.03 | 0.023 | 0.117 | 0.04 | C3 D3 A1 B1 | | |
| Optimal combination | | | | | | | |
| | | | | | A1 B3 C3 D1 | | |

Note: A, HYP (%); B, Ultrasonic power (w); C, F68 concentration (%); D, Oil / Water (v/v)

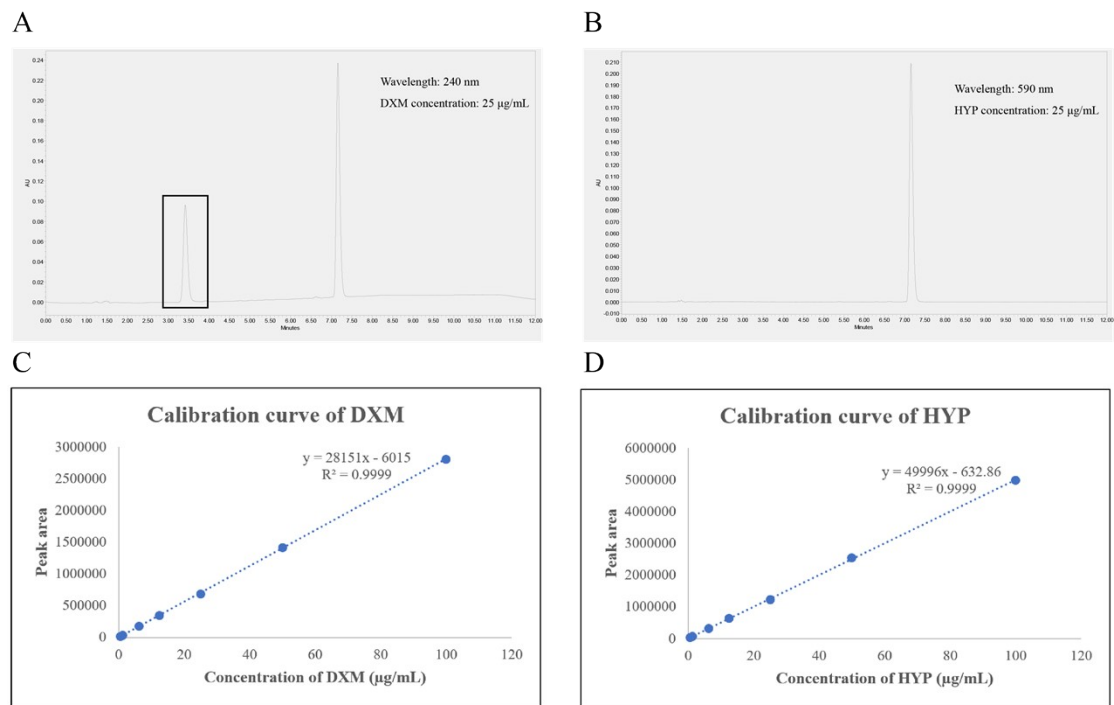


Fig. S1 Chromatogram and Calibration Curves of HYP and DXM. (A) Chromatographic peak of DXM and (B) chromatographic peak of HYP. (C) Calibration curves of DXM and (D) HYP.

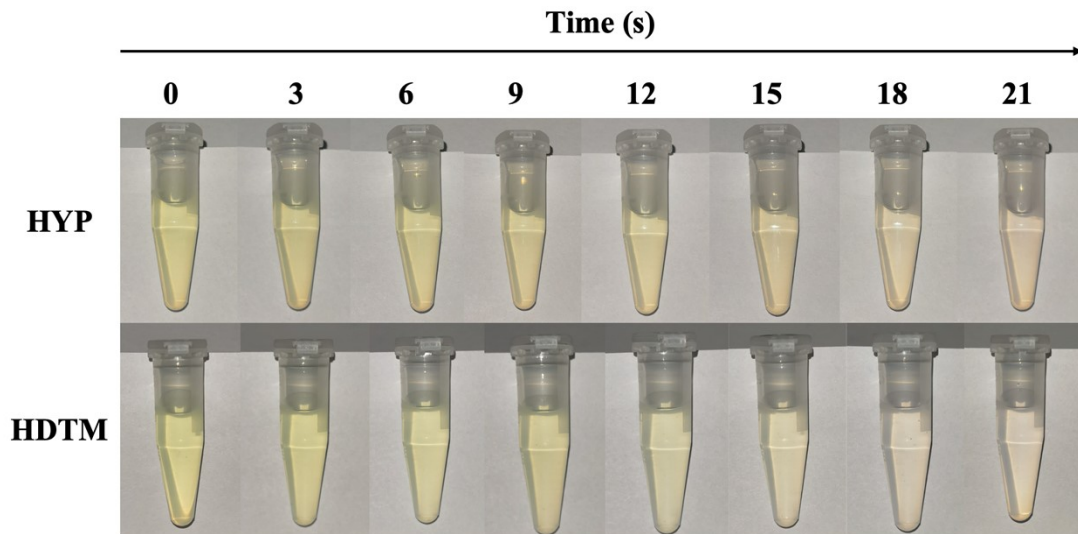


Fig. S2 The fading process after DPBF reacts with ROS produced by HYP.

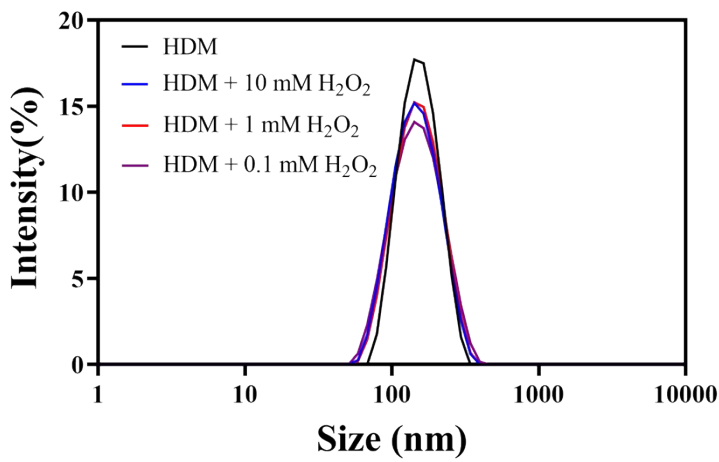


Fig. S3 Particle size changes of the HDM in response to various ROS conditions.

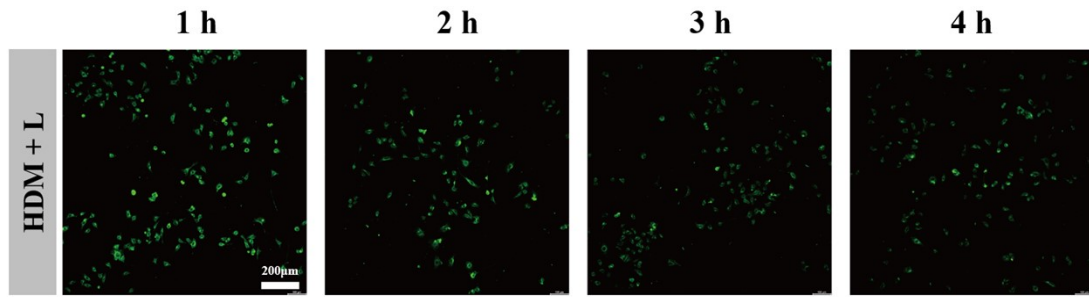


Fig. S4 Fluorescence analysis of intracellular ROS produced by HDM in 4T1 cells.

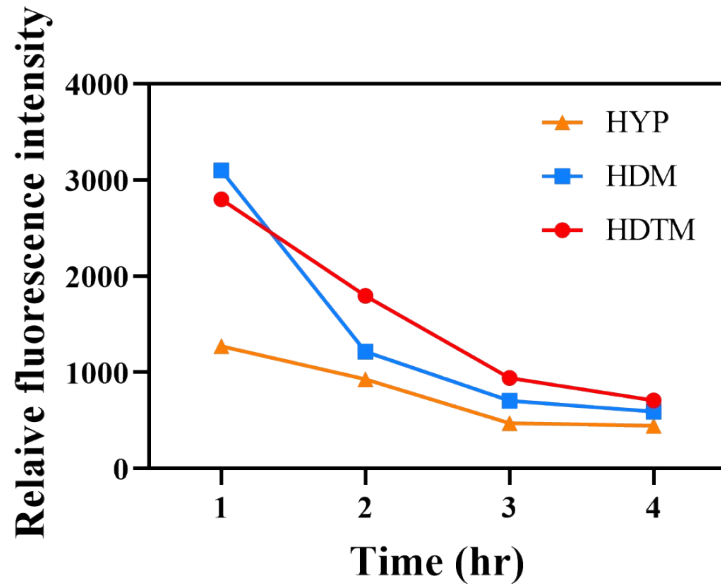


Fig. S5 Quantitative analysis of intracellular ROS produced by HYP formulations in 4T1 cells.

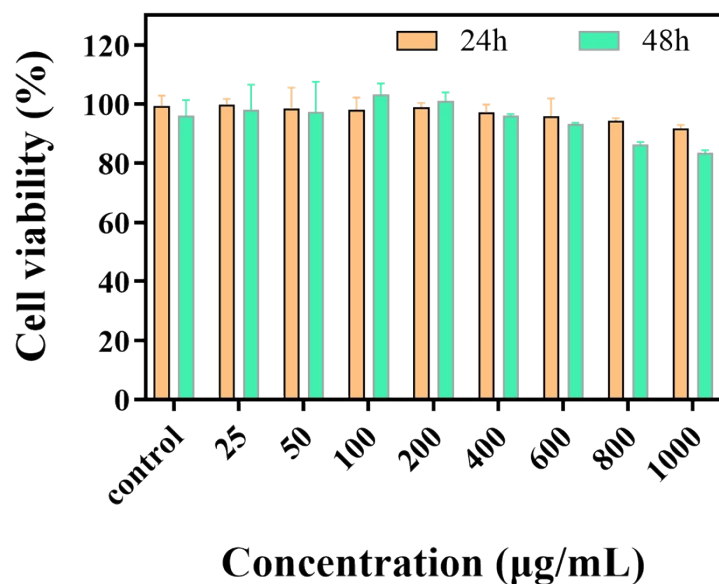


Fig. S6 The cytotoxicity of polymer PLGA_{10k}-TK-PEG_{2k} in 4T1 cells determined by MTT assay (n=3).

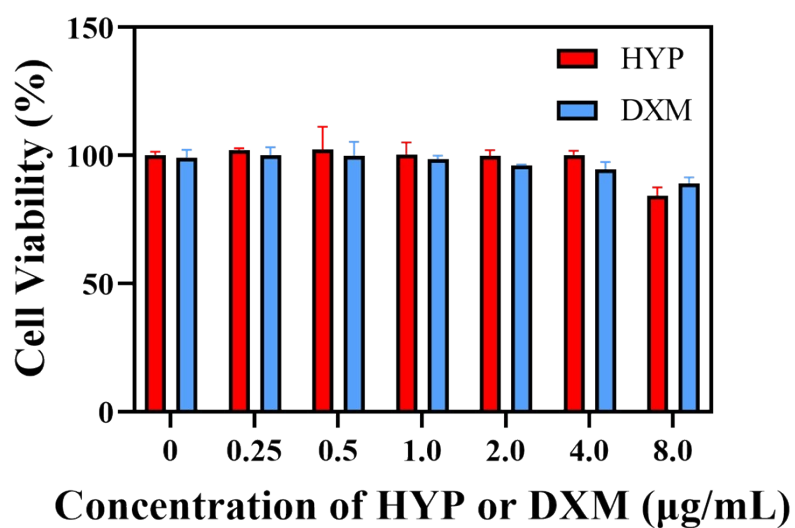


Fig. S7 The cytotoxicity of HYP and DXM in 4T1 cells determined by MTT assay (n=3).

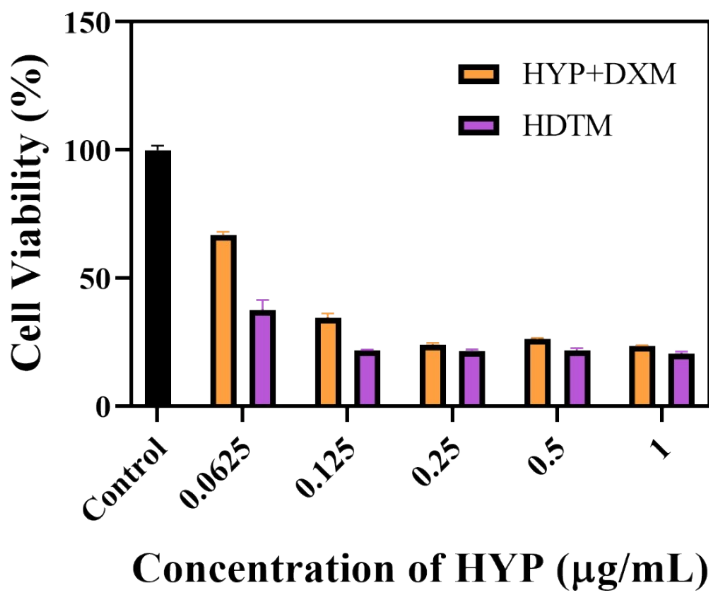


Fig. S8 Phototoxicity of HYP formulations in B16 cells determined by MTT assay (n=3).

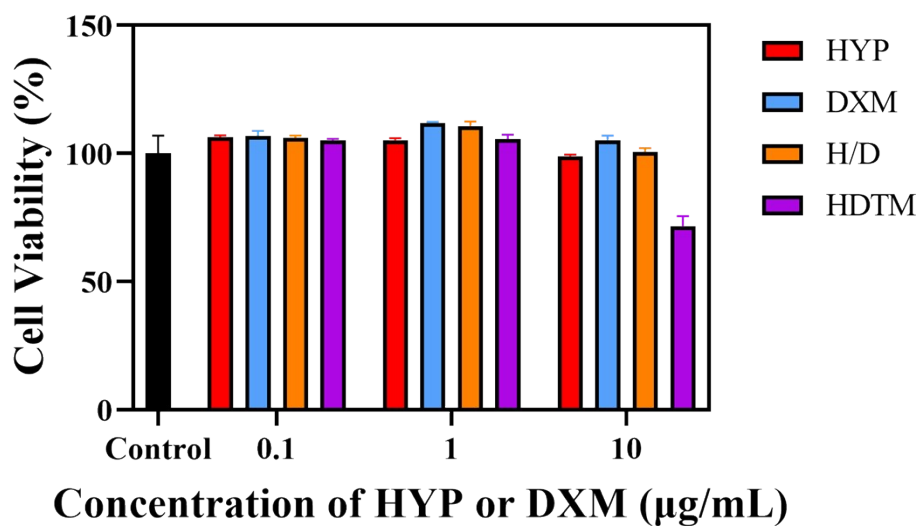


Fig. S9 Cytotoxicity of DXM and HYP formulations in HUVEC cells determined by MTT assay (n=3).